



Conducting AFM on graphene

THESIS

submitted in partial fulfillment of the
requirements for the degree of

BACHELOR OF SCIENCE

in

PHYSICS

Author : Ruben van Erkelens
Student ID : 1437267
Supervisor : Jan van Ruitenbeek, Federica Galli
2nd corrector : Thijs Aartsma

Leiden, The Netherlands, July 4, 2018

Conducting AFM on graphene

Ruben van Erkelens

Huygens-Kamerlingh Onnes Laboratory, Leiden University
P.O. Box 9500, 2300 RA Leiden, The Netherlands

July 4, 2018

Abstract

This thesis deals with the use of conducting AFM to image the topography and conducting properties of graphene on SiO₂. Specifically, the current image will be used to distinguish graphene from SiO₂ and the height image to identify the edge of the wafer. These together can show how far graphene reaches this edge. For testing the usability of the Conducting AFM module measurements were also made on gold and on graphite. Lastly, specific settings were tested and discussed for optimal current imaging results.

Contents

1	Introduction	1
2	Theory	3
2.1	Graphene	3
2.2	Nanogap junction	5
3	Fundamentals of AFM	7
3.1	Atomic Forces	7
3.2	Principles of AFM	8
3.3	AC mode	10
3.4	Conducting AFM	12
3.5	Current preamplifier	13
3.6	Force/distance- and current/distance-curves	14
3.7	I/V spectroscopy	16
3.8	Quantitative Imaging mode	16
3.9	AFM probes	17
3.10	AFM setup	19
4	Results	21
4.1	AC Edge Measurements	21
4.2	QI Edge Measurements	22
4.3	CAFM on Gold/Mica	23
4.4	CAFM on Graphite	25
4.5	CAFM on Graphene/SiO ₂	27
4.6	QI CAFM Settings	34
4.7	Conclusion	37

Introduction

A material that is 200 times stronger than steel, 1000 times lighter per square meter than paper, with a theoretical electron mobility 10^7 times higher than that of copper and being only one atom thick sounds very promising for many scientific purposes [1]. This material exists, and it is called graphene. Ever since its discovery in 2004 by Novoselov et al.[2], who won a Nobel prize for their work, physicists have recognized the potential of graphene and have done a considerable amount of research on it. The amount of articles published on graphene has been rising exponentially ever since its discovery.[3]

At Leiden University in the group of Van Ruitenbeek, Sasha Vrbica and Amadeo Bellunato (G. Schneider, LIC), are working on creating a nanogap junction. This is a junction consisting of two silicon oxide wafers with atomically sharp graphene on top. The wafers are set at less than a nanometer apart from each other, so that tunneling current can go through the graphene on one of the wafers, crosses the gap, and goes through the graphene on the other wafer. One exciting possible application for the future is to use the nanogap junction as a DNA sequencer. It works by "holding" a DNA string in between the two wafers, measuring the change in output current for each part of the DNA, and therefore reading the coding of the DNA. Doing this will not be easy though, as there are practical problems in developing a well controlled nanogap junction. One is that the graphene must be sufficiently close to the edge of the wafers. The reason is that even when the wafers are close to each other, if the graphene is too far from the edge, the distance between the two graphene sheets will be too far for current to be able to tunnel through. It would be helpful to be able to identify if the graphene reaches the edge, before or during work with a certain wafer. The main aim of the project is to use the Atomic Force

Microscope (AFM) to distinguish graphene from the underlying silicon oxide. Conducting AFM could be used to overcome the short-comings of Tapping Mode/Phase Imaging. Specifically, this is done by mapping the conductivity and the height over a certain area on the wafer. Graphene, being a semi-conductor, and silicon oxide, an insulator, can therefore be distinguished. At the same time, the height will be measured, and thus can be identified where the edge of the wafer is. By comparing the height image with the conductivity image, one may see how close the graphene is to the edge. More will be told about this in chapter two, where the workings of the AFM, the central tool for this project, will be explained. Also, several measuring modes which prove to be useful will be explained in chapter two, one being QI mode, which is an essential mode for doing Conducting AFM (CAFM). Some theory about graphene and a more in depth view on nanogap junctions will be given in chapter one. Results and measurements on different materials, such as gold and graphite for testing, and graphene, will be shown and discussed in chapter 3, together with some tests in several CAFM settings.

Theory

2.1 Graphene

Graphene is a two-dimensional material completely consisting of carbon atoms, structured in a hexagonal lattice, each 1.42 Angstrom apart, which originates from graphite. Graphite is way more common than graphene, it can be found in nature and it is a mineral crystalline form of carbon. Graphite is a layered material. Sheets of graphene themselves seldom break, and are even reported to be 200 times stronger than steel.[4] In graphite the layers are kept together by weak van der Waals bonds, therefore they can be easily separated. One can make graphene by exfoliation, that is, by using sticky tape on graphite, taking a few layers off. Doing this over and over again can leave a few layers or possibly even one layer of graphene. This method was first reported to work by Geim and Novoselov, who successfully isolated graphene and characterized its properties, for which they won the Nobel prize in 2004.[2]

Some of the electronic properties of graphene shall be further explained here, as well as some relevant theory about electron bands. Graphene consists of carbon, which has six electrons, of which four are available for chemical bonding. Due to the hexagonal structure of graphene, a carbon atom has 3 neighbours with which it can bond its electrons. These electrons are in the s orbital and are called core electrons and the electron that is left is in the π orbital and is called a delocalized electron. Because the Pauli exclusion principle states that identical fermions (so electrons) cannot occupy the same quantum state, they will all have different energies. At absolute zero temperature all states will be occupied and the highest energy state is at the Fermi energy by definition. In semi-conductors and insulators, the valence band is the highest range of energies with occu-

pied states at zero temperature. A band with higher possible energy states exists, and is called the conduction band. Valence band and conduction band are separated by a band gap in which no states are possible. Metals have no band gap, and therefore have one band containing both occupied and unoccupied states. At temperatures higher than zero, thermal energy can excite delocalized electrons, moving them up to a higher electron state. This leaves an unoccupied lower energy state called a hole. Metals have no band gap, meaning that this can happen with relatively low energy excitations. Insulators have a band gap which is generally too great to overcome, meaning that electrons will not occupy higher energy states. Semi-conductors do have a band gap, but this band gap is relatively small. With an excitation energy that is great enough, the band gap can be overcome, moving an electron up to the conduction band. These excited electrons are referred to as free electrons and they are free to move through the material or fill up an existing hole. Free electrons will move in a certain direction once a bias voltage is applied, giving a current. The possibility for flow of electrons is what makes a material conducting. Doping of a semi-conductor can further increase conductivity, by using impurities with possible energy states in the energy range of the band gap of the semi-conductor.

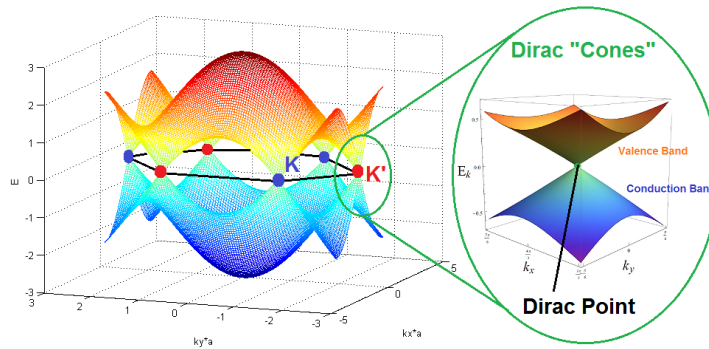


Figure 2.1: Dirac cones of graphene at six hexagonal separated points in a energy-momentum spectrum. Copyright: muonray

Due to the dispersion relation for electrons in graphene, the valence and conduction bands each form a cone at six hexagonal separated points in a energy-momentum spectrum. At these points, called Dirac points, the cones go linearly with respect to energy, meaning that valence band and conduction band touch. The result is that graphene has no band gap, thus behaving like a metal, but the two bands do not overlap, thus behaving like a semi-conductor. Furthermore, the linearity of the cones at the Dirac

points gives a relation between energy and momentum by: $E = \pm v_F |p|$ [5] with E and $|p|$ the energy and absolute momentum of the electron respectively and $v_F = 8 \cdot 10^5 \text{ m/s}$ the Fermi speed. This formula has similar form as the relativistic formula for massless particles moving with the speed of light, where the speed of light c is replaced by v_F . Thus, electrons near valence band to conduction band energy effectively behave as massless particles. A result is that graphene has a very high electron and hole mobility, theoretically $200,000 \text{ cm}^2 \text{ V}^{-1} \text{ s}^{-1}$, which is 10^7 times higher than that of copper. Practically, this mobility is less due to the substrate on which the graphene lies. On SiO_2 substrates the theoretical limit becomes slightly less to $40,000 \text{ cm}^2 \text{ V}^{-1} \text{ s}^{-1}$. [6]

2.2 Nanogap junction

With electronics becoming smaller and smaller, one can imagine the importance of junctions at the nanoscale in electrical circuits. Nanogap junctions can also be used though for measuring the resistance of molecules by placing them in between the electrodes of the junction. Though nanogap junctions are often consisting of two metal electrodes, there are definitely reasons to look at graphene as a material for electrodes. Graphene is thinner than metals, making it possible to measure on smaller molecules. DNA being a good example, where graphene is thin enough to measure on each nucleotide individually, without the next nucleotide bothering the measurement, thus becoming a DNA sequencer. The process in which these graphene nanogap junctions are made, matters a lot for the quality of the junction. The graphene on the junctions of interest for this project were made with a process called Chemical Vapor Deposition (CVD).

This method is more practical, faster and enables to make more graphene than the exfoliation method. It works by keeping a gas high in carbon, such as methane gas, in a container, then graphene can form with the help of a catalyst, such as copper. High temperature is needed to start the dissociation of carbon atoms and to make them form graphene. The copper is removed by dissolving it, and the graphene sheet is transferred onto a silicon/silicon oxide substrate. This is the process of CVD on graphene. [1] The substrate is mainly silicon, but the borders of the substrate react with oxygen and form silicon oxide. Silicon oxide is a well known insulator, and makes a good material to combine with graphene. The graphene cannot be placed onto the substrate in a way so that it reaches the edge, as it is done manually, so another method is needed to get the graphene as close to the edge as possible.

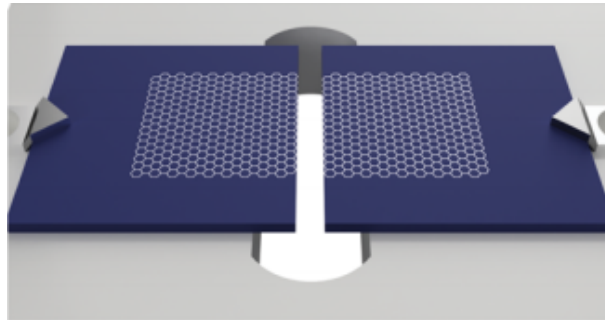


Figure 2.2: Schematic view of two wafers with graphene (white) on top.[7]

A solution is to place two wafers close to each other, placing a sheet of graphene on top of them supported by a polymer coating (polycarbonate) to make it possible to bridge the gap. In the gap, the graphene is then removed by H_2 plasma etching and the polymer is all over removed by dissolving it in chloroform.[7] This should leave two wafers with graphene up to the edge, as seen schematically in figure 2.2. However, the etching also removes some of the graphene close to the edge, with the possibility of graphene being several nanometers away from the edge. Several nanometers can be too much for tunneling, as the current in tunneling decreases exponentially. AFM can help identify the graphene to see how far away from the edge the graphene really is.

Fundamentals of AFM

3.1 Atomic Forces

An Atomic Force Microscope (AFM) measures the atomic Forces between a very sharp probe (AFM tip) and the surface of the sample to produce a high resolution image of the sample surface. Atomic forces are the short range interactions experienced as neutral molecules or atoms get close to each other. There are several atomic forces to consider. Firstly, there is the Coulomb repulsion force; as atoms get closer to each other, their respective electrons will repel each other for having the same charge sign. The second force follows from the Pauli exclusion principle. The Pauli exclusion principle states that two electrons cannot occupy the same quantum state, this means that if two atoms are so close to each other that their electrons are almost overlapping each others orbitals. If a shell is full, no more electrons can be added, because then electrons would have the same state. The result is a repulsive force.

Other atomic interactions are the Keesom force, Debye force and London dispersion force. These come from the interaction between dipoles. A molecule which has atoms with different electronegativity, has a charge imbalance and is called a permanent dipole. The interaction between permanent dipoles is called the Keesom force. The Debye force is an interaction between a permanent dipole and an induced dipole on a otherwise charge balanced molecule. It occurs when the electrons of a non-polar molecule get attracted by the permanent dipole, making it an induced dipole. Lastly, there is the London dispersion force, or also called an induced dipole-induced dipole interaction. It originates from the probabilistic nature of electrons due to quantum mechanics, as electrons can temporarily take positions that make two adjacent atoms temporary dipoles.

Molecules with more electrons will have a higher associated London dispersion force. No permanent dipoles are needed for this interactions and therefore this interaction occurs with all molecules. All together, the forces approximately follow the Lennard-Jones potential

$$U(r) = ar^{-12} - br^{-6}$$

And the force, being its negative derivative, given as:

$$F(r) = -\frac{dU(r)}{dr} = 12ar^{-13} - 6br^{-7}$$

Here U is the potential, r the distance between two molecules or atoms and a and b two constants. Figure 3.1 shows what this potential and force looks like.

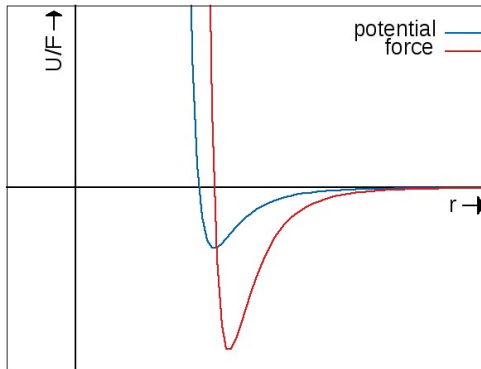


Figure 3.1: Lennard-Jones potential (blue) and its corresponding force (red)

From the point where the force goes from attractive to repulsive (so U at a minimum), two molecules or atoms are said to be "in contact".

3.2 Principles of AFM

The AFM is a scanning probe microscope, meaning that it acquires images by letting a probe move over a surface in a raster motion. This probe consists of a cantilever with a tip at the end which is a few nanometers in diameter. Depending on the distance from the tip to the surface, the cantilever bends due to the Van der Waals Forces between the tip and the the sample as $F = -kd$ (Hooke's Law). This deflection (d) can be detected

by using a laser and a photo diode detector. The laser points at the cantilever, of which it reflects towards the photo diode detector, so when the cantilever deflects, the laser path will be different. Laser alignment is necessary each time a new tip is mounted or when the laser position is off due to thermal drift. The photo diode detector has four quadrants, each quad-

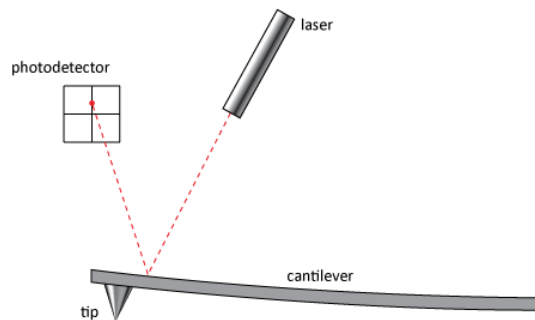


Figure 3.2: A laser reflects off the deflected cantilever onto a photo diode detector. From: <https://www.doitpoms.ac.uk/tlplib/afm/cantilever.php>

rant generates a current which is proportional to the area of the quadrant which is illuminated by the reflected laser spot. The output current of the photo detector is converted to a voltage. This voltage is proportional to the (vertical) deflection, and the proportionality factor is called the "sensitivity" of the photo diode detector and needs to be known to convert voltage to nm. When the deflection d is known in nm, also the force can be determined using Hooke's law $F = -kd$ and the elastic constant of the cantilever k . The probe will move over the sample in the X and Y direction while the force is kept constant (in constant force mode). This way a relative height image over a certain area can be made. Movement of the probe is regulated by piezo elements in X,Y and Z direction. Applying a voltage to these piezos make them extend or retract in the corresponding direction, this way the position can be precisely changed. A Z-motor stage is used specifically to approach to a position close enough to the sample surface so that the probe is ready for measurement. The tip needs to get really close to the surface in order to measure and yet not bump into it with great force, since this might break it. PID feedback (Proportional, Integral and Differential feedback) controls the approach by checking the force working on the probe. This force is compared to a force setpoint set by the AFM user, this way the tip can approach the sample surface accordingly. When in approached state, feedback is still on to correct for vertical displacements happening due to changes in environment. Also when measuring, the height differences in the surface make it so that the

force changes and therefore the position of the probe changes. Feedback corrects these changes depending on the mode used. The most classical mode for the AFM is contact mode, where the tip experiences an amount of force to make contact with the sample surface. The feedback does this by continuously changing the tip-sample distance so that the force remains constant. The changes are proportional to the topography of the surface, and therefore the height is mapped.[8] One might prefer contact mode for its simplicity, however there are definitely advantages to other modes. Some other modes and their advantages and features shall be discussed in the next sections.

3.3 AC mode

A common problem with contact mode is that the tip and sample both experience high lateral and vertical forces, due to being so close to each other. This can severely damage the sample or make the tip blunt and distort the image. On biological/soft materials, the tip can damage or displace the sample. A solution is to oscillate the cantilever, making the tip come in contact only a short duration, and thus not exerting that much force over a long period of time. In standard AC mode the cantilever is oscillated around its resonance frequency with an amplitude which is large enough so that the tip will be in contact with the surface and then immediately out of contact again.

The cantilever can be represented by a driven, damped harmonic oscillator:

$$m\ddot{x} + c\dot{x} + kx = F_0e^{i\omega t}$$

with x the displacement, m the cantilever mass, c the damping coefficient, k the spring constant of the cantilever, $F_0e^{i\omega t}$ the driving force represented as a driving force amplitude F_0 and a complex exponential dependent on angular frequency ω and time t . This equation can be solved for the amplitude of the cantilever:

$$A(\omega) = \frac{F_0/m}{[(\omega_0^2 - \omega^2)^2 + 4\gamma^2\omega^2]^{1/2}}$$

with $\omega_0 = \sqrt{k/m}$ the natural angular frequency, which is the angular frequency of the system when no damping or driving force is present, and $\gamma = \frac{c}{2m}$ the damping factor. As the cantilever gets in contact with the sample, the atomic forces working on the cantilever increase, which act like a

damping force, thus also increasing the damping factor γ . From the formula for the amplitude it can be seen that an increased damping factor results in lesser amplitude. The resonance frequency, which can be found by taking the derivative of the expression for A and setting to zero, yielding $\omega_r^2 = \omega_0^2 - 2\gamma^2$, decreases with increasing damping factor. Also, the phase difference between driving force and cantilever oscillation, given by $\phi = \tan^{-1}[\frac{2\gamma\omega}{(\omega_0^2 - \omega^2)}]$, increases or decreases depending on the sign of the denominator as damping factor increases.[9] Differences in the amplitude and phase of the cantilever from those of the driving force are what is measured to make an image. The amplitude is used as a setpoint for feedback in AC mode. The described effect can be seen more clearly in figure 3.3.

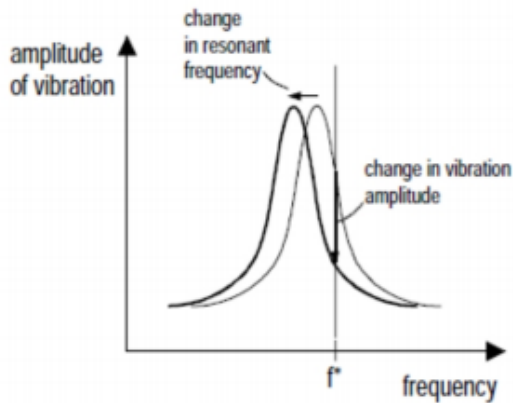


Figure 3.3: Amplitude change and change in resonance frequency in the repulsive regime (tip in contact).[10]

During approach the z-piezo position will keep moving downwards until the amplitude is small enough so that this setpoint is reached. During imaging, the amplitude is kept at the constant value of the setpoint by changing the z-position. This position is then translated to the height in the topography image. The measured phase is also valuable information, as the phase changes 90 degrees at resonance frequency and there is a dissipation induced phase change when the tip is in contact. This can be used to determine a difference between materials, since the height profile might not show a significant difference when going from one material to the other when these two materials have the same height, but the phase will change more rapidly. This method can also be used to distinguish graphene from silicon oxide, though not further investigated in this thesis. AC mode is hard to use in combination with Conducting AFM, be-

cause the contact time is too short and the Conducting AFM preamplifier is not fast enough to measure in this short time. More about this will be said in section 3.5.

3.4 Conducting AFM

An application of main importance for this thesis is Conducting AFM (CAFM). During CAFM, a voltage difference is applied between sample and tip. When the (conducting) tip is sufficiently close, a current will run between tip and sample first because of tunneling, and then because of direct contact. The current will then go from the tip to a preamplifier (preamp), which is used to amplify this current and turn it into a voltage so that it can be measured. Because the cantilever deflection and the current through the cantilever are measured independently, both a topography and current image are acquired at the same time. The topography image is made as usual with the mode used, the current image is made by translating the measured voltage back into a current for each x,y position. Some conditions should be met if a current is to go from sample to tip; First of all, the tip and surface should be in contact, so that they are in series. How long the tip is in contact depends on the measurement mode used. In theory, at small distance from contact a tunneling current would run through, however in practice this current is almost negligible in comparison with the current achieved right after when snapping into contact. More on the current distance behaviour in section 3.6. Secondly, the sample surface should be conducting. The higher the conductivity of the material the higher the current. Measuring different currents at different locations can therefore be a way to distinguish materials and in particular graphene and silicon oxide. It should be noted though that contamination can make the surface of a normally conducting material insulating. Adsorbate are a form of contamination which is harder to avoid, it consists of molecules in air which tend to stick to the sample. Longer exposure to air can increase the amount of adsorbate on a sample and therefore decrease the conductivity and the reliability of CAFM. Lastly, the tip should also be conducting. Oxidation and contamination are similarly a problem here as for samples, therefore using clean tips is similarly a solution. High currents can also make the tip blunt, that is why a current decreasing resistance is often used in series with the bias voltage to keep the current low.

3.5 Current preamplifier

In CAFM, the output is very small (nA) current. This means a preamplifier is needed to amplify and translate the current into voltages. A basic preamplifier circuit scheme for CAFM is given in figure 3.4[11] This is a so called trans-impedance amplifier and is similar/identical to the one used for Scanning Tunneling Microscopy (STM).

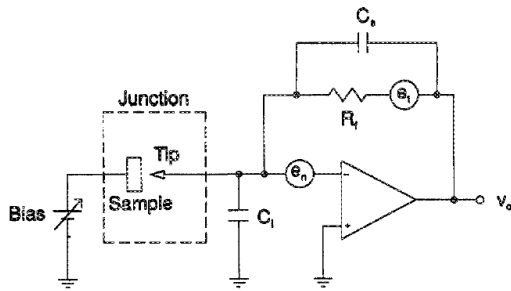


Figure 3.4: Circuit of a preamplifier used in CAFM.

At the left of this circuit, a bias is applied to the sample, if the conditions for CAFM are met, then a current will flow to the tip. The first nuisance is in the form of a shunt parasitic capacitance, C_i . This capacitance comes from the wires from the tip to the preamp. This can be minimized by minimizing the distance from tip to preamp. The operational amplifier (opamp) in the preamp has a noise voltage source, e_n , depending on the characteristics of the opamp. There is a feedback resistor R_{fb} , and with it a parasitic shunt capacitance C_s associated to the resistor. Next in the circuit the thermal noise (Johnson noise), e_t , is given by $e_t = \sqrt{4k_B T R_{fb} f}$, it is caused by thermal motion of electrons in a resistor, with k_B the Boltzmann constant, T the temperature, and f the frequency range. Finally, the preamp will give an output voltage V_o . Its value depends on all the previous components, however if one was to consider an ideal preamp without noise, the output voltage would be given by: $V_{out} = -I_{in} R_{fb}$. The current is amplified to a voltage by a factor of $-R_{fb}$, which is called the gain of the preamp.

The greater this value, the higher the amplification. Note that in the formula for the Johnson noise, the noise increases with the square root of R_{fb} , whereas the total output voltage increases with R_{fb} linearly. This leads to a better signal to noise ratio. The feedback resistance should not be taken too high though, because it also decreases the bandwidth. The bandwidth cut off frequency is given by: $f = 1 / \sqrt{2\pi C_s R_{fb}}$ [12]

It is desired to have an as high as possible signal to noise ratio, yet a wide enough bandwidth range to measure in. The CAFM by JPK used for this thesis uses a value for the resistor of $10^8 \Omega$, and has a bandwidth up to $1 - 2 \text{ kHz}$. [13] Measuring with a frequency higher than the bandwidth frequency, will decrease significantly the output signal out of the preamplifier. This would be the case for AC mode, as the frequencies of the tips used to make high quality images in AC mode are much higher than 2 kHz (usually around 70 or 300 kHz). Also, to prevent tip wear, the tip in AC mode does not go very deep into the sample, meaning that it is in contact only very shortly. This makes AC mode suboptimal for CAFM, because the short contact and high frequency combination would give a very poor signal to noise ratio. Either contact mode or, as discussed in section 3.8, QI mode can be used, since they both measure in a low enough frequency range or slow enough.

3.6 Force/distance- and current/distance-curves

Force/distance-curves (F/d-curves) or current/distance curves (I/d-curves) can give a lot of valuable information. They describe how the force and current react as the tip comes closer to or moves away from the sample. An example of how a F/d-curve can look like is figure 3.5.

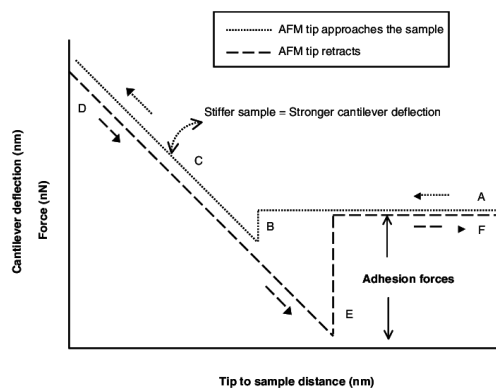


Figure 3.5: Force/distance-curve [14]

From A to C the probe approaches the surface (probe extends). D to F is called the probe retract. The probe starts at A at a position out of contact, and then approaches the sample. At B the tip snaps into contact because of the attractive Van der Waals forces and (in ambient) capillary forces. At C the repulsive forces of the sample build up and make the can-

tiler deflect by $F = -kx$. With an infinitely stiff sample, the decreased distance (which is not really a distance anymore as tip and sample are in contact) is completely compensated by the deflection (so the sample is not deformed/indented), the slope of the F/d curve then gives the spring constant of the cantilever. However, a realistic sample forms a spring as well, the decreased distance is compensated both by a deformation in the sample and a deflection of the cantilever. The slope gives the combined spring constant. The force keeps increasing with decreased distance until a force setpoint is reached, after which the probe is retracted back. When retracting, starting at D, the behaviour is different from probe extend/approach as atomic and adhesion forces prevent that the tip comes out of contact, but eventually, when using enough force to retract, the tip will go out of contact. The adhesion forces are non-conservative and come from a water film which is always present on surfaces in ambient. The water on the sample surface tends to stick around the tip and pull it down as it retracts, causing a bent of the cantilever. Using soft cantilevers will keep the tip in the water for a longer distance and if the water film is thicker, the adhesion forces will be higher. When getting sufficiently far away, so at E, the tip comes loose and it is out of contact (F).

Just like the force, the current is very much dependent on the distance from tip to sample. At great distance there is no current, the tunneling distance is too large. However as the distance gets very small, say in the order of nanometers, a current will start to run, even though tip and sample are not in contact yet. This is the tunneling current, coming from the quantum mechanical nature of electrons, as they have a probability to cross the potential wall of the gap between tip and sample. Its current has an exponential dependence on the distance. The tunneling current is very small in comparison with the current when in contact but it can be measured by the preamp if set on a very high gain ($10^8 - 10^9$). It should be noted however that measuring the tunneling current can be difficult, because one would have to keep the tip sufficiently close the sample but not yet in contact.

Right after snapping in contact, the contact area can be seen as the contact area without any load on the tip. Further load by pushing deeper into the sample can increase contact area, thus further increasing the current. When contact is established and if the contact is "clean", the preamp needs to be set at much lower gain settings.

3.7 I/V spectroscopy

Once in contact, the force can be kept constant by the feedback in AFM mode*. Now, changing the bias voltage will change the current. Measuring the current over a range of voltages is called current/voltage (I/V) spectroscopy. Figure 3.6 shows a typical I/V curve. The linear slope is directly related to the resistance R in case of Ohmic contact, which is essentially the resistance experienced from sample to tip. If the current exceeds the saturation level of the preamplifier the measured current becomes constant as soon as the saturation current is reached.

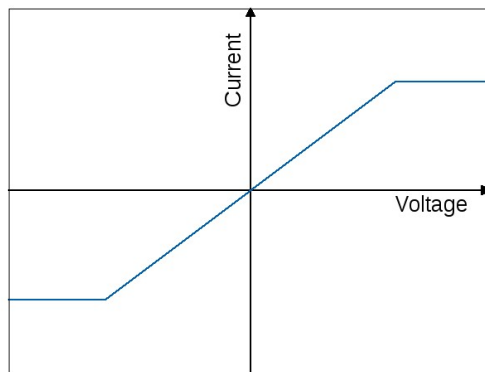


Figure 3.6: Example of an I/V spectroscopy curve. The curve is linear in the middle and thus shows Ohmic behaviour. With increasing/decreasing voltage the measured current increases/decreases respectively until saturation of the preamplifier is reached. The current will remain constant afterwards.

3.8 Quantitative Imaging mode

Quantitative Imaging mode (QI mode) is a relatively new mode introduced by the company JPK Instruments AG.[15] A JPK NanoWizard 3 was used for the experiments of this thesis, and so has QI mode been used for numerous measurements. In QI mode a force/distance-curve is made at every pixel. In order to do this, the tip has to cover a certain distance range at each pixel. Unlike AC mode, the cantilever of the probe is not driven to oscillate. It is in fact the whole tip holder that is moving up and down at lower frequency (max. 2kHz). Just like how F/d-curves are normally

*Note that this is different than STM-spectroscopy. In this case the feedback is disabled, when the STM probe is at a given distance.

made, the probe extends until a force setpoint is reached. At which distance this setpoint is reached, is then translated to be the height of the image. The probe goes back to the retracted position, moves towards another pixel, and measures again. Repeating for each pixel in a raster results in an image. Imaging with QI does usually take slightly longer than imaging with tapping mode or contact mode, because of the time it takes to make a force/distance curve at each pixel. With this slow pixel taking, comes a low measuring frequency. This makes it ideal for doing CAFM, because the frequency is nicely in the range of the bandwidth of the preamplifier and therefore the preamplifier has enough time to perform an accurate current measurement for each given pixel. Of course, contact mode CAFM could also be used, however QI CAFM does not have the disadvantages of high lateral and vertical forces, because it is only temporarily in contact at every pixel. Contact mode is known to cause much high tip wear of the conducting coating.

3.9 AFM probes

The choice of probe can make a significant impact on image quality. In this section, different kinds of probes will be covered. AFM probes consist of a chip, with a cantilever attached to it. This cantilever should be reflecting when using a laser spot as measuring tool. At the end of the cantilever is a tip. Tips can have a pyramidal or hemispherical shape, depending on the type/manufacturing, or irregular/not defined shape. One can imagine that a probe with a sharp tip will make an image with a higher resolution than one with a blunt tip, as the resolution is very much determined by the tip radius. Probes can furthermore vary in resonance frequency, dimensions, stiffness, and material. Most probes are made out of silicon or silicon nitride. On different samples and in different modes, different probes are optimal for use.

In contact mode, the cantilever should be quite soft, so with a low spring constant. A cantilever high spring constant would apply a lot of force on the sample, which could damage it or viceversa, on a hard sample the tip apex would become more and more blunt. The resonance frequency is low, as can be seen from the formula for a harmonic oscillator: $f_{res} = 1/2\pi\sqrt{(k/m)}$ The spring constant can be determined from the geometry of the cantilever: $k = \frac{Ewt^3}{4L^3}$ with E the Young's modulus, which is an elasticity constant of the material (, for silicon it is around $150GPa$) and w , t and L respectively the width, the thickness and the length of the cantilever.[16]

In AC mode, it is often beneficial to use cantilevers with a higher resonance frequency (about 70 – 300 kHz). This can mean a high spring constant, but it depends on the material choice. High frequency (stiff) cantilevers experience less negative effects from adhesion, as the cantilever would go in and out of the water film present in ambient air during AC mode, the high spring constant would make the cantilever push through the water more easily. In AC mode, the frequency of the cantilever also greatly influences the scanning speed as the resonance frequency is directly linked to the measuring frequency.

The choice of probe in QI mode is not as significant as it is in tapping mode, as most probes can be used for height imaging purposes. However, one might want to avoid very soft tips when measuring in very humid conditions, because as said before, they suffer more from adhesion. This adhesion can dominate the whole F/d -curve, giving a qualitatively bad pixel. Also, the cantilever experiences a small oscillation as the tip shoots out of the water, this is called mechanical ringing. Oscillations are of bigger amplitude when soft, low frequency cantilevers are used, but stiff cantilevers might keep oscillating for a longer time. As for all modes, there should also be looked at the material one is measuring, as soft samples get damaged more easily by a probe with a high spring constant than hard samples do.

For CAFM, there is in particular one very clear and important condition to be met: the tip should be conducting. Silicon or silicon nitride tips are not conducting. These tips could be used, if they are coated with a layer of conducting material. A disadvantage to this approach though, is that this coating can wear off during measurements, especially when using high forces, leaving contact points with silicon or silicon nitride. There are also probes which are made of conducting material themselves, so that they can measure current without further coating. A good example is the so called "Rocky Mountain" probe, produced by the company Rocky Mountain Nanotechnology, LLC.[17] These probes consist of a platinum wire on top of the chip. This wire functions as the cantilever, with at the end a platinum tip. Advantages to these tips are that platinum is a good conducting material and the whole tip is made out of it so there is no problem from it wearing off. Also, the tips are quite sharp, especially when compared to coated tips, as the coating layer significantly increases the tip radius, resulting in less resolution. However, the wire cantilever is relatively soft, with a resonance frequency between 4.5 – 105 kHz. This might cause the tip to bend while measuring with high forces, which results effectively in a blunt tip. The softness also causes it to suffer more from adhesion, as described above.

3.10 AFM setup

Every AFM apparatus is different in the details, but all AFMs have conceptually many of the same components. The AFM setup shall here be explained with figure 3.7, which is the AFM by JPK used for this thesis.

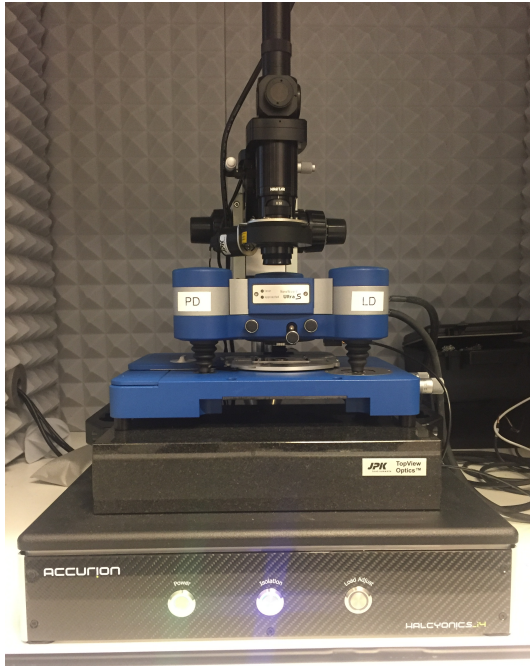


Figure 3.7: AFM setup

The measuring component of the AFM is seen in blue, with under it the blue sample stage. The laser is inside the AFM. It reflects from a mirror, through a glass cantilever holder, onto the cantilever. Then it reflects back, goes through the glass, towards a photo diode detector inside the AFM. The laser path is illustrated in figure 3.8. Above the AFM stands a top-view optical microscope with a CCD camera, which is needed for finding the probe, aligning the laser spot on the cantilever or finding a certain area on the sample. The black stage underneath (Accurion) actively damps vibrations that may distort the image. The AFM is positioned inside an acoustic isolation enclosure, which also keeps the environment inside steady, as temperature differences can have a big impact on subsequent measurements in the form of thermal drift. Thermal drift can cause the parts of the AFM to move with respect to each other, negatively influencing imaging with distortions. The AFM is connected to the controller

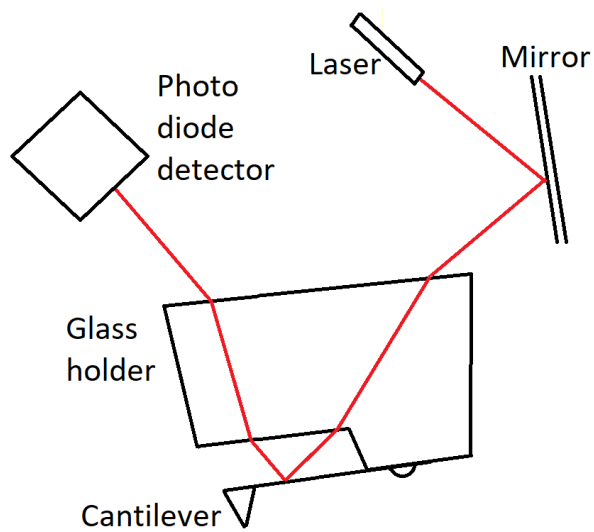


Figure 3.8: Laser path in the AFM

and software on the computer can then do acquisition and further analysis on the data.

Results

In this chapter AFM measurements will be shown and discussed. That is, firstly, measurements on the edge of a graphene/Si/SiO₂ sample, both in AC and QI, without CAFM. Then, CAFM measurements on different materials, such as Gold on Mica, graphite, and graphene on Si/SiO₂. Also, the different settings for optimizing CAFM imaging will be discussed with the help of images. A graphene/Si/SiO₂ sample was used with a SiO₂ thickness of 290nm, as this improves the optical visibility of the sample[18].

4.1 AC Edge Measurements

As for the general goal of this project, the measurement on the edge of a sample is quite important. In the AFM image it should be possible to see a clear macroscopic drop of what should be the edge. For this particular set of measurements, a graphene on Si/SiO₂ wafer was used, similar to the one used in the nano junction. Firstly, the edge is measured with AC mode. A typical result can be seen in figure 4.1.

The edge is clearly visible, before the edge the image is brown/white colored, after the edge black. The image appears as being featureless, this is because the height scale includes the drop-off, so details are not visible on this color scale. The measured height difference is shown, though this is not the actual height difference from the top of the sample to the bottom, it is simply the height at which the probe does not go down any further. The probe has a maximum movement range of 6.5 μ m once approached, however the position of the tip is usually somewhere in the middle of this range, this explains the apparent height difference of 2.3 μ m. For this reason, it is important to start with the tip on top of the sample and go

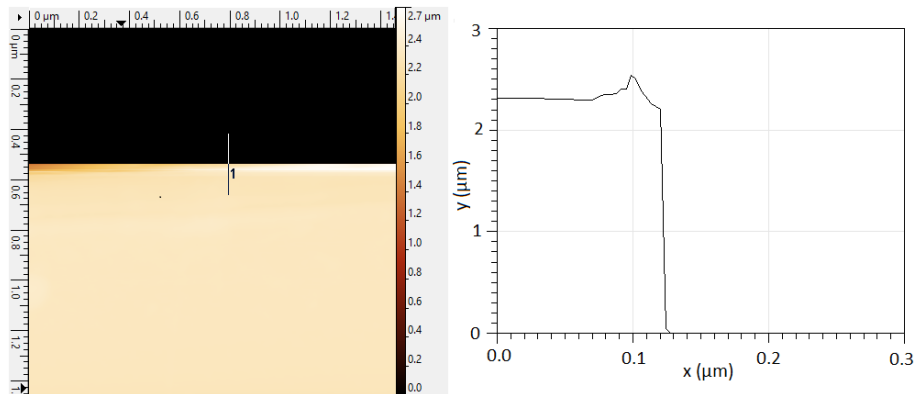


Figure 4.1: AC edge measurement. The left is the AC height image, the right is the height change over the drawn line. The image was made on a graphene/Si/SiO₂ wafer, with a 209kHz silicon tip.

downwards, instead of starting beyond the edge and onto the sample, as in this case the tip will bump into the sample edge, and as the edge is higher than $6.5\mu\text{m}$, the tip will crash and get damaged.

4.2 QI Edge Measurements

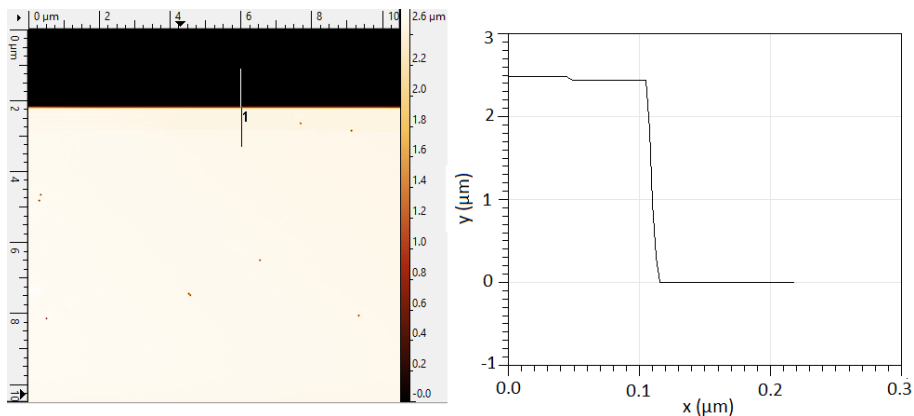


Figure 4.2: QI edge measurement on a graphene/Si/SiO₂ wafer with a straight drop off. Tip (209 kHz) and sample are similar as in figure 4.1.

Though AC works for edge measurement, the edge measurements must also be possible in QI, because QI should be used for doing conducting AFM. The same wafer as in figure 4.1 was used, a resulting image is shown

in figure 4.2. Both QI and AC images look very similar and are both able to measure the edge effectively.

4.3 CAFM on Gold/Mica

All further shown figures and measurements with CAFM were measured with RMN-25Pt300B tips[17], which have a characteristic resonance frequency of 20kHz. For testing the usability of CAFM, a sample of gold on mica* was used. Gold is a well known conductor. Taking that into account, and the consideration that the gold film did not show cracks and is continuous all over the substrate, whereas graphene might leave gaps, makes it so that gold is a promising material for testing the CAFM module.

As F/d, I/d-curves would show, figure 4.3, current could be measured on this material, though its values would differ significantly, to the point of not being measured at all. The maximum/minimum current which could be measured is +/- 12nA, which is the saturation level of the preamplifier, which means that the actual currents going through the tip were higher than this value when saturated. The inconsistency in current measurements could be explained by the tip having to make a clean contact with the sample surface, which is not always realized everywhere on the tip, because of adsorbates forming on the tip and on the gold. During measurement the tip can both lose or gain adsorbates as the tip moves over the surface during imaging, or penetrates the surface during an F/d, I/d-curve. In the case of the left graph in figure 4.3, the current shoots up to saturation right after contact was reached, meaning that the tip makes a relatively clean contact with the gold.

When it comes to imaging gold, one would expect to see atomically flat terraces at which the gold is raised up slightly higher or lower. This is a characteristic structure for Au(111) surface on mica substrates. In figure 4.4 one can see these terraces more clearly.

Also, a current image was made, where it is visible that there is more current measured at spots where there is a slope in height. An explanation can yet again be found with the contact area between the tip and the sample; a flat surface will only be in contact with the very end of the tip, while a slope will be in contact with the sides of the tip as well. There might even be contamination on the end of the tip, while the sides of the tip are clean. The gold sample which was used has been in air for several weeks,

*Mica is an insulating mineral which, similar to graphite, can be easily cleaved in atomically flat layers.

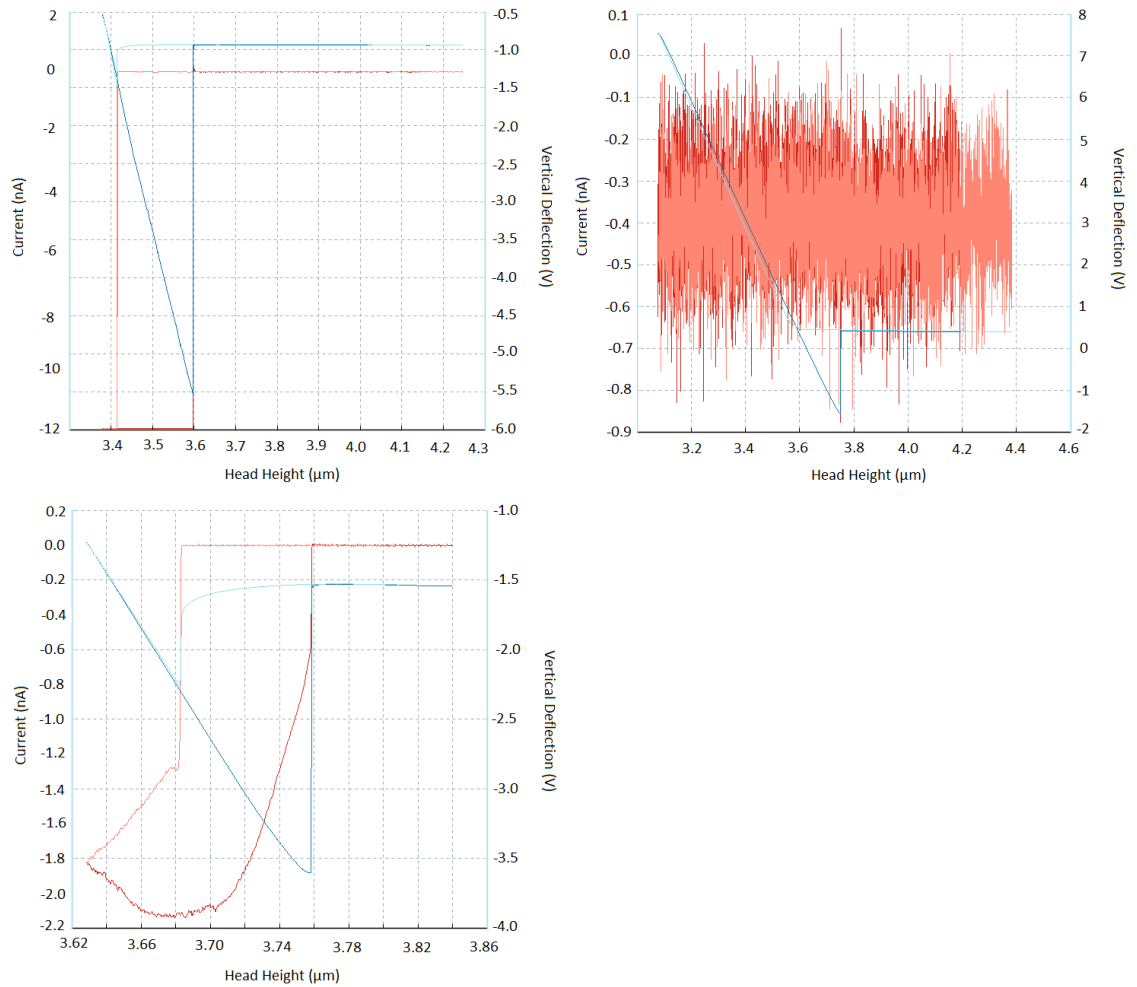


Figure 4.3: A set of three F/d , I/d CAFM measurements, $V_b = -10V$ (a voltage this high should generally be avoided, as it can destroy the tip, here it was naively used in order to measure more current). Top left: The current goes to the saturation level of $-12nA$ immediately after the tip gets in contact. Top right: The gold and tip fail to get clean contact, and the measured current is just the noise level of the preamplifier. Bottom: Slightly more clean contact is reached right at first contact, after which contact area increases gradually together with the measured current up to $-2.2nA$.

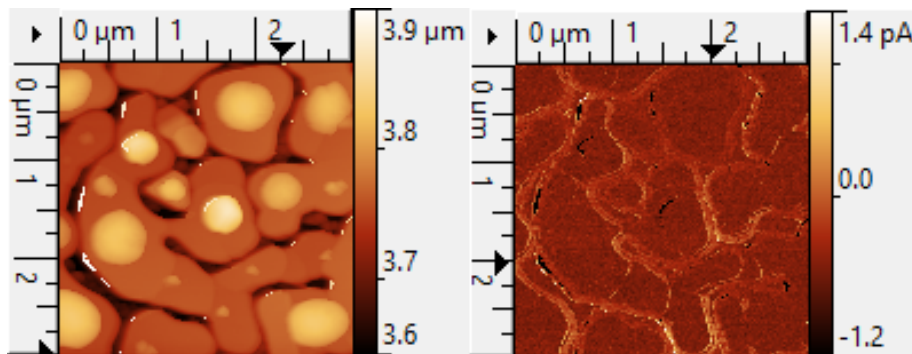


Figure 4.4: QI CAFM measurement on gold, $V_b = 1.108V$. Left: Height image showing terraces of gold. Right: Current image. More current is measured at black gaps in the height image, due to the change in height at these spots. The current in this image is very small, just $1.4pA$ max. Contamination is a possible explanation for this small current.

meaning that many adsorbates have formed on top of it, making it hard to measure current. This explains the rather low value of current measured.

4.4 CAFM on Graphite

By taking a sticky tape, and removing the top layers of a graphite sample, a new clean surface is created. The sample surface is now clean and less contaminated. This means that there should be current measured all over the sample. Typical for graphite are its steps in which a layer goes one or more atomic layer higher. Figure 4.5 shows an example of two such steps. One step of $5nm$, which indicates that the step increases in several layers, and one step which can hardly be seen at first sight. Last step increases about $0.3nm$ in height, which compared to the theoretical $0.335nm$ inter-layer distance[4], means that this could be an increase of just one layer. The current at a step is higher due to the slope of the step, increasing contact area. The bigger step has a bigger contact area, thus higher current than the small step. This is confirmed by the measured current peaks of $5nA$ and $2nA$ of big and small step respectively, as seen at the bottom right graph of figure 4.5.

Figure 4.6 shows an F/d , I/d curve for graphite. It has the peculiarity that the current increases way before the tip seems to be in contact with the graphite, over $6\mu m$ before. What is very likely to have happened is that a graphite flake caught onto the tip while measuring before this particular curve. The conducting graphite flake enables current to go through way

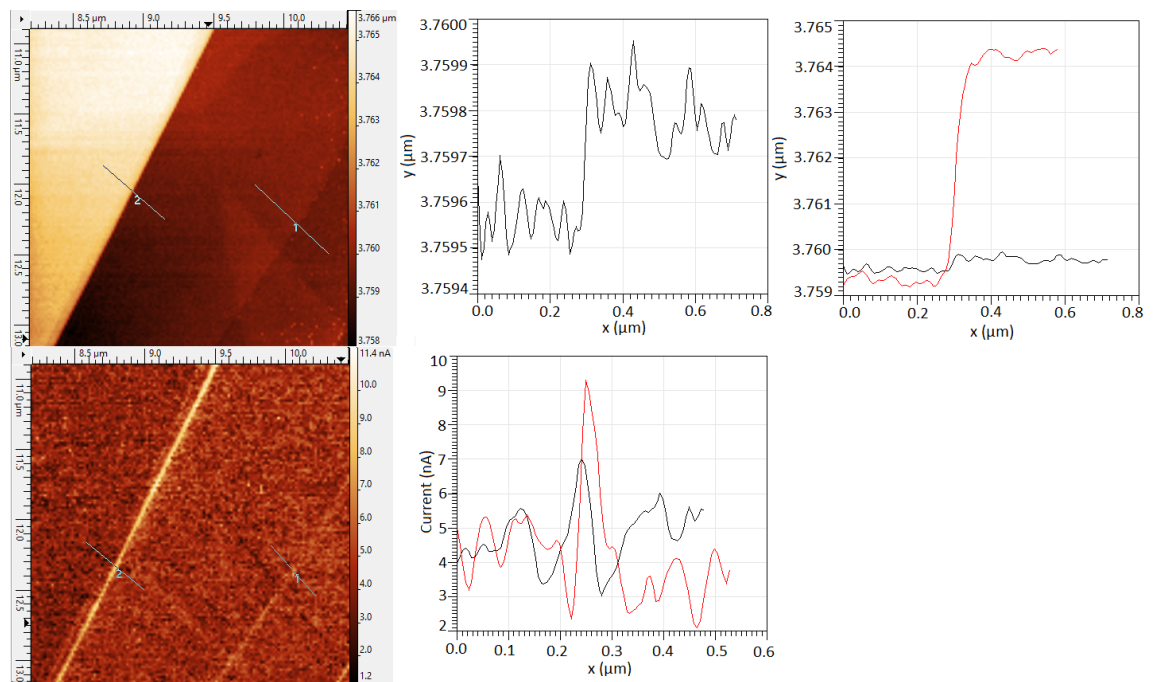


Figure 4.5: QI CAFM measurement on graphite, $V = 0.608V$, force setpoint: $sp = 33nN$. Top left: Topography image with two steps. Top middle: Height difference of the small step, corresponding to line 1 in the topography image. The step height is about $0.3nm$. Top right: Height difference of both steps. The black curve (line 1) is much smaller than the red curve (line 2) of the big step. The latter corresponds to a height difference of about $5nm$. Bottom left: Current image with the steps visible as white lines with higher current. Bottom right: The current of the small step (black, line 1) increases with about $2nA$ and of the big step (red, line 2) increases with about $5nA$.

before the tip is even close. This happened often because it is quite easy to pick up flakes while scanning on graphite.

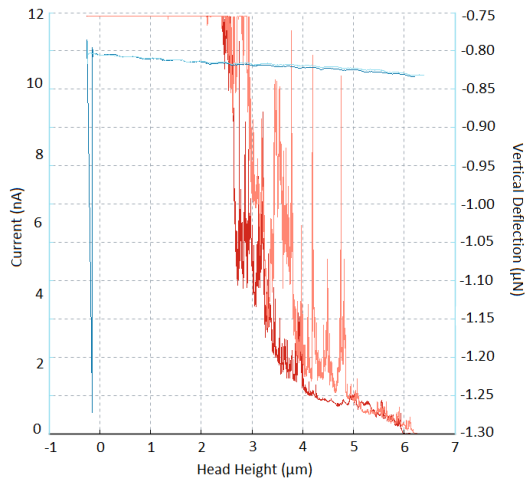


Figure 4.6: *F/d, I/d curve on graphite, $V_b = 0.608$. The current increases way before the tip reaches contact with the graphite, could indicate that a flake is attached on the tip.*

4.5 CAFM on Graphene/SiO₂

It is apparent that it is very well possible to make proper CAFM images, though it remains the question whether the method is applicable on graphene for the purpose of this project and what is the resolution of CAFM. One problem of graphene which is not present with graphite is that the graphene should be all over from the place where the bias is connected to the location where the tip lands. Graphene being a mono layer material can show discontinuities and cracks in several places. This is also the case for full coverage graphene. A sample with a relatively uncracked surface would be optimal. Another disadvantage of measuring on graphene in comparison to graphite is that it is obviously not possible to take off a top layer with sticky tape, and therefore the graphene sample should be very clean from the start and should be kept at vacuum to avoid adsorbates to form on the surface.

The samples that were used were made by CVD in G. Schneider's group at LIC. For these samples, a thickness of SiO₂ of 290nm was used. This thickness was chosen to improve the optical visibility of graphene. The three layers of the sample (graphene, SiO₂ and Si) have different refractive indexes and so interference happens depending on wavelength

and material thickness. A SiO_2 thickness of $280 - 300\text{nm}$ was shown to be optimal for visible light.[18] One can imagine that a monolayer material can otherwise be hard to see and find, yet it can be very beneficial for experiments if one could locate the graphene prior to measuring. The improved visibility would prove useful for locating the boundary from graphene to SiO_2 with an optical microscope before measuring on this boundary. This can be seen in figure 4.7.

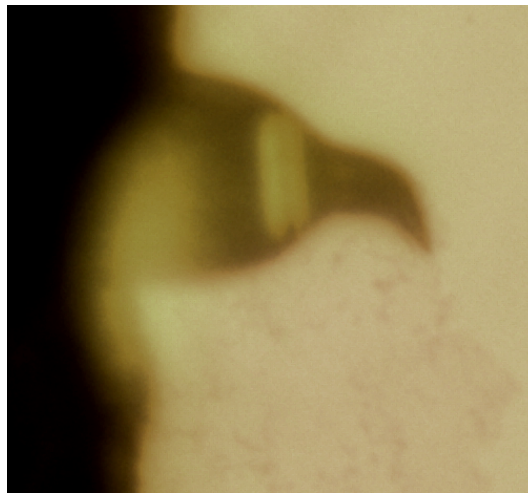


Figure 4.7: An optical picture of the tip and the sample made with yellow light. The graphene can be seen in principle optically due to the chosen SiO_2 thickness of 290nm of the sample. The SiO_2 appears as plain yellow while the graphene is slightly darker and more patchy. In fact what helps the most here to see graphene is the defects and folds which are present in this graphene prepared in this way. By spotting this the boundary from graphene to SiO_2 can be found. The RMN probe has a tip that bends off downwards, as can be seen as a black "pigeon" in the middle of the picture. On the far left a part of the tip holder is visible in dark black.

The graphene appears as darker and patchy, the SiO_2 shows no characteristics and is plain yellow through the microscope.

In the course of measurements on graphene, a modification in preamplifier was made. The reason is that because most images would show currents of saturation values, the preamplifier had to be changed in order to gain more information from the image. By decreasing the gain resistance with a factor 50 from $10^8\Omega$ to $2 \cdot 10^6\Omega$, the saturation level was increased with a factor 50, making it possible to measure currents up to 600nA . A disadvantage of this is that decreasing the gain resistance im-

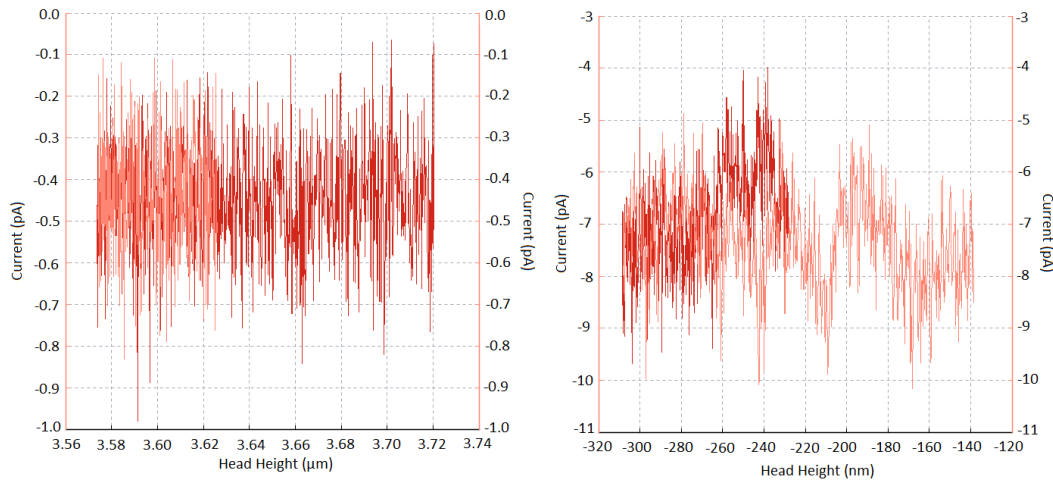


Figure 4.8: *I/d* curves of preamplifier noise. Left: Before the preamplifier modification. The noise has an impact of approximately 0.8pA . Right: After the preamplifier modification. The noise has an impact of approximately 6pA , meaning that the noise has increased with a factor 7.5 due to a factor 50 gain resistor decrease.

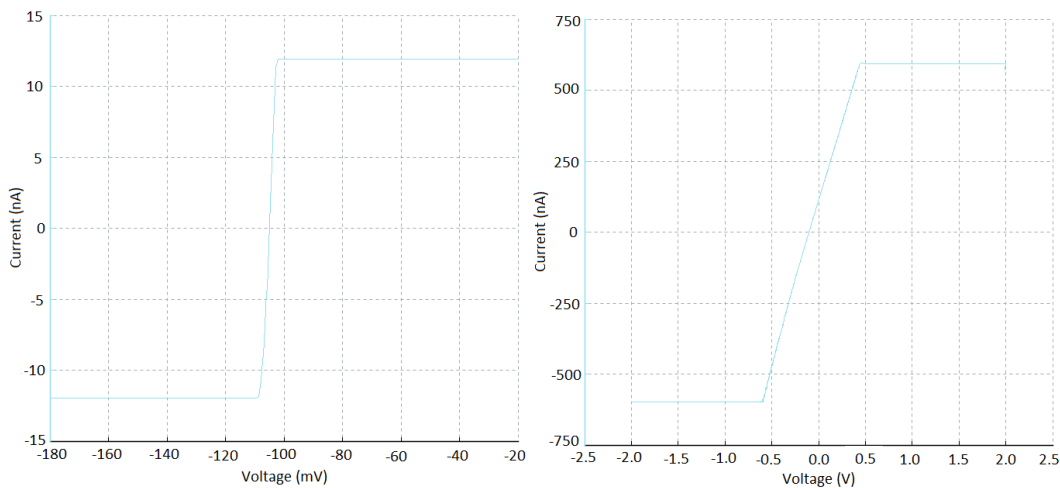


Figure 4.9: *I/Vs* made on graphene, with a typical linear slope. There is a voltage offset of -0.108V . $sp = 70\text{nN}$. Left: curve made before the preamp switch, with $\pm 12\text{nA}$ as saturation level. $R = 276\text{k}\Omega$ Right: curve made after the preamp switch. The current reaches up to 600nA . $R = 889\text{k}\Omega$

poses more noise. Comparing the noise in the F/d , I/d -curve of the new preamp settings with the old preamp settings shows that there is a significant change in noise, but the noise with the new preamp settings is still just in the range of a few pA , which does not matter when measuring on currents in the range of nA , as seen in figure 4.8.

I/V s on graphene, figure 4.9, show that the current can reach the saturation level of $\pm 600nA$ with the new preamp, at about $\pm 0.5V$ away from the offset voltage of $-0.108V$. In the I/V with the old preamp settings, the current reached saturation as shortly as $0.04V$ away from the offset. This is not a factor 50 apart, which is because the resistance experienced by the current is different in both I/V s. This could have been calibrated using a known resistor. The resistances in both images, as can be received by the slope by $V = IR$, are $276k\Omega$ and $889k\Omega$ for left I/V and right I/V respectively.

To interpret these values, an estimate of what can be expected for the resistance and current on graphene was made. The total resistance of the system can be seen as a sum of the resistance of the point contact between tip and substrate, and the resistance of the substrate between tip and location on the substrate where the bias is applied. The latter being negligible for the thick and well conducting gold and graphite substrates, but graphene is atomically sharp, so this resistance should be taken into account. Taking a homogeneous resistivity ρ , the resistance of an Ohmic resistance can be calculated by the formula

$$R = \int_{l_1}^{l_2} \frac{\rho}{A(l)} dl$$

with l_1 and l_2 the starting and ending lengths as seen from a reference point, and $A(l)$ the cross sectional area dependent on length. In the particular case of a sheet of graphene, the resistance can be calculated with circular sections, where each circular section has radius l , width dl , and thickness t . The sections are in series, and can thus be calculated by integrating over dl . The area is given by $A(l) = 2\pi lt$. Then, using the definition for sheet resistance $R_s = \rho/t$ and filling in the area, the expression for R becomes:

$$R = \frac{R_s}{2\pi} \int_{l_1}^{l_2} \frac{dl}{l}$$

Taking l_2 as the tip radius, and noting that the tip on average was about $0.1\mu m$ further into the sample than at point contact, then using a SEM-image of an RMN tip[17], it can be roughly estimated by $l_2 \approx 200nm$. l_1 is the length from (the middle of) the tip to where the bias is applied, which

can be estimated as $l_1 \approx 1\text{cm}$. The sheet resistance for graphene was taken as $R_s = 1840\Omega \approx 2 \cdot 10^3\Omega$ [19]. Filling in then gives $R = 3k\Omega$.

To complete the estimate, the resistance from the point contact is added, which can be seen as a contact of an individual atom. For one atom this is the quantum resistance $R = \frac{h}{2e^2} \approx 13k\Omega$ [20]. It is here assumed that a one atom contact is made, but it should be noted that this might not be the case for a tip pushed into a sample. Adding up the estimate for the sheet graphene and the point contact gives $R = 2 \cdot 10^4\Omega$. Comparing this estimate with the results from figure 4.9 gives that the estimate is 17 and 56 times smaller than the resistances of $276k\Omega$ and $889k\Omega$ of left and right curve respectively. A voltage of $V = 0.5V$ corresponds to saturation current, $600nA$, for the right curve, but would give a current of $3 \cdot 10^2A$ using the estimate.

There are several possible explanations for the difference in estimate and measurement. Firstly, the chosen value for the sheet resistance could have been different from that of the measurements. The sheet resistance varies strongly depending on the state of the graphene used, because the amount of cracks and adsorbates could be different in every graphene sample. Secondly, the chosen lengths were estimated very roughly, especially the radius of the tip. However, the terms for length are in a logarithm after evaluation of the integral for resistance over circular sections and so differences in the chosen lengths will only matter little.

Finally, images on the boundary from graphene to SiO₂ were made. Some of the CAFM images of the graphene to SiO₂ transition are shown in figures 4.10 and 4.11. The transition is clearly visible in both the current image and the height image. In the conducting image current is measured on the graphene and then suddenly stops, thus when reaching SiO₂.

Another way to check whether or not this is the transition is by looking at the height increase when going to graphene. Figures 4.10 and 4.11 show a height increase of near and about $2nm$. This is not in accordance with the theoretical $0.335nm$ [4], for this should be the thickness of a single graphene sheet. The reason could be air and water molecules which are trapped under the graphene sheet. During the creation process of the graphene/Si/SiO₂ wafer, the graphene sheet was laid on top of the SiO₂, however there might have been molecules on the SiO₂ which could not escape. This adds to the measured height difference. $2nm$ is actually a height difference more often measured with AFM on graphene.[21]

In figure 4.10 and 4.11, a streaky pattern is visible in the current image when coming onto graphene, after a while this pattern suddenly stops and high current is measured. The tip measures an image like this starting from the bottom right horizontally. When finished with a horizontal line it

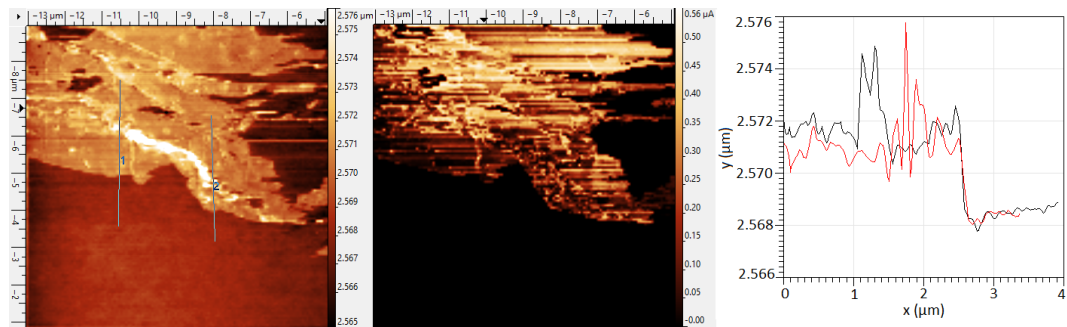


Figure 4.10: QI CAFM measurement on graphene made after the preamp modification. $V_b = 0.108V$, $sp = 92nN$ Left: A topography image where the top half has a part which is slightly higher than the rest of the image. Middle: Current image. The upper part is graphene, as current is measured there, whereas no current is measured on SiO_2 . On the right side of the current image there appears to be no/little graphene, which is also visible in the height image. Right: Two height differences of around $2nm$, with a small peak which could be contamination. black: 1 red: 2

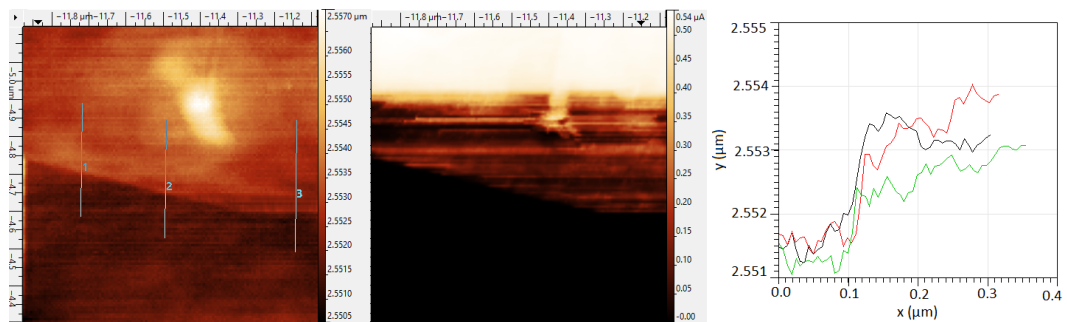


Figure 4.11: QI CAFM measurement on graphene after the preamp modification. $V_b = 0.108V$, $sp = 92nN$ Left: Topography image. The upper part is slightly higher. Middle: Current image. The upper part is graphene as seen in this current image. No current is measured on the bottom part. Right: Some height differences in the graphene to SiO_2 transition. The differences are around $1 - 3nm$ black: 1 red: 2 green: 3

goes up one line. During this process the tip could lose or gain some dirt, thus explaining a streaky pattern. The high increase in current in figure 4.11 could be explained by a loss of a relatively high amount of dirt from the tip. With current above saturation level, further small loss or gain of dirt of the tip will remain unmeasured and no streaky pattern is seen. On the right side of figure 4.10 there appears to be little or no graphene. The graphene seems to be damaged there, which could possibly have been caused mechanically by the tip during measurement.

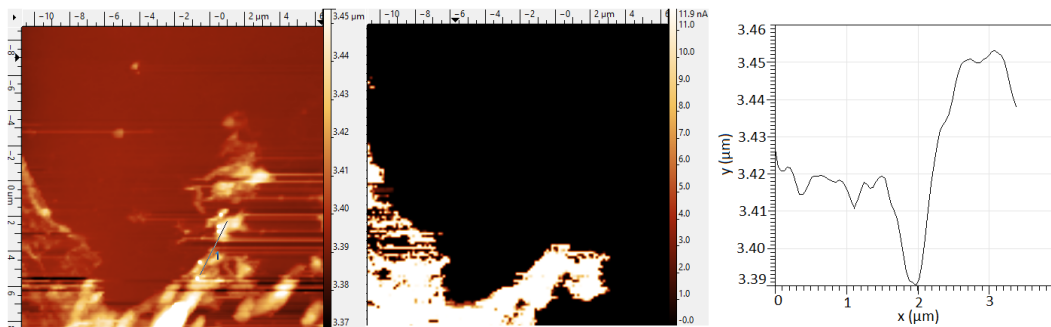


Figure 4.12: QI CAFM measurement made before the preamp modification. $V_b = 0.608V$, $sp = 120nN$ Left: Topography image. Middle: This current image seems quite similar to the height image but for one part which is not "recognized" in the current image. This could be an island of graphene loose from the bulk. Therefore this island was not in contact with the bias. Right: Height over the line drawn in the height image. A clear gap is visible, giving a distance between bulk and island of around $0.2 - 1\mu m$.

In these images it is possible to recognize graphene just in the topography image. This is also the case in figure 4.12, however in this image a feature in the middle of the image is visible where the height image shows an island next to the bulk graphene. This cannot be SiO₂ as this is typically flat, nor does it look like contamination. It could be a graphene island which is loose from the bulk. In this way there is no electrical contact with the island, therefore no current is measured on it.

As the current image follows the topography image so closely, one could wonder why CAFM is even necessary in the first place, because topography images show the graphene to SiO₂ transition sufficiently well in previous shown measurements. The answer is that the height image alone is not enough when looking at the graphene to SiO₂ transition in the same image as the edge measurement of the wafer. The reason is that the graphene to SiO₂ height difference of few nanometers is negligibly small in the height image when compared to the drop off of the edge of several micrometers, making the transition near to invisible, see figures 4.1

and 4.2. The CAFM module should be able to show the graphene to SiO₂ transition together with an edge measurement.

However this measurement was not done, because samples degraded rapidly due to increasing contamination and adsorbates. Even when stored in vacuum, current on graphene appeared to be unmeasurable in a timespan of four weeks. Note that samples were stored at about *1mbar*, so not in high vacuum.

4.6 QI CAFM Settings

Lastly, optimal settings will be discussed for measuring on graphene with the CAFM module. Settings were tested by making images with different settings and comparing them.

A setting that can make a significant change to a current image is the bias voltage. The bias voltage can be set from $-10V$ to $10V$, though voltages this high can destroy the tip, which makes sense as a too high current will go through a tip of a few nanometers radius. Also, a voltage that is too high will mostly show either saturation level of current at conducting spots or no current at all at non-conducting spots. For seeing more detail in images, one would want to see a wide range of different currents all through the image, so that different areas can quantitatively be compared. A low voltage serves this purpose well, however using a lower voltage results in a current relatively smaller to noise levels. Figure 4.13 show several used voltages of $0.008V$, $0.108V$ and $0.308V$. Even at the lowest voltage of $0.008V$, the pattern can be seen. This voltage is arguably enough, though a voltage a bit higher, such as $0.108V$, can show differences more clearly. Voltages of $0.308V$ appear to be unnecessary, but also to change both current and topography image. Figure 4.13 shows a strongly changing topography image on subsequent measurements, which is possibly caused by the tips movement during measurement. The current images show a streaky pattern similar as in figure 4.11, which could again be caused by losing and gaining dirt on the tip visible in the current in lower current images. In the second to third current image there is an increase in voltage applied, yet a decrease in current measured. This could yet again be explained by the loss or gain of dirt on the tip, as the amount of dirt could change while measuring on SiO₂ as well.

Which force setpoint should be used greatly depends on the level of contamination on sample and tip. This is because a high force will push the tip through layers of contamination or adsorbates, making sure contact is reached. This means that the optimal setpoint greatly depends on the

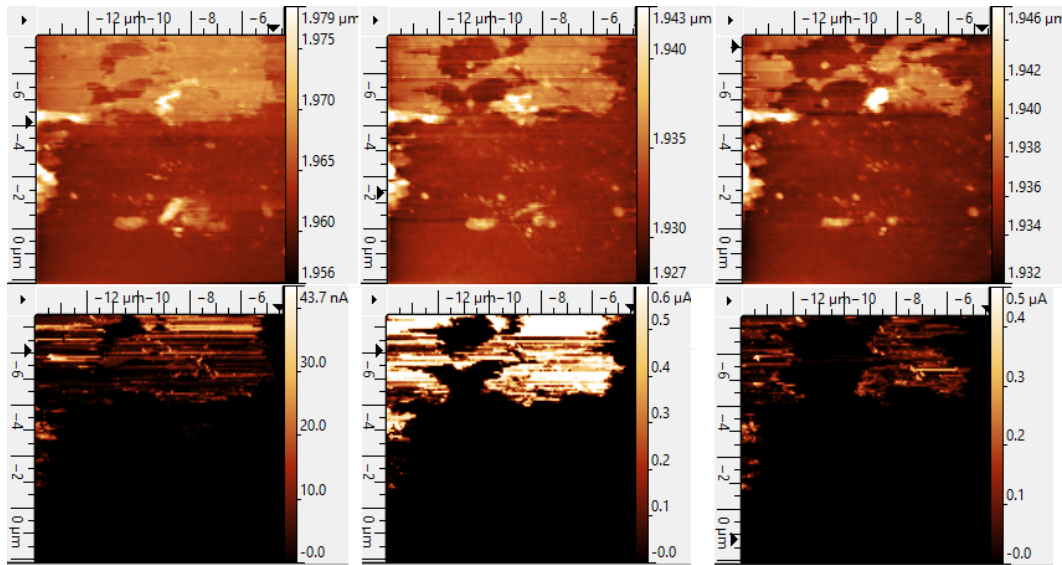


Figure 4.13: QI CAFM measurement on graphene, $sp = 90nN$. Top: Topography images. Bottom: Current images. From left to right: $V_b = 0.008V, 0.108V, 0.308V$.

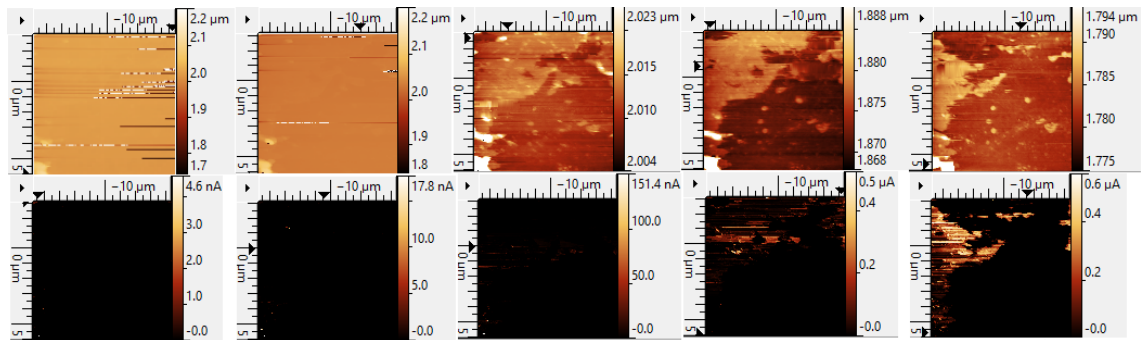


Figure 4.14: QI CAFM measurements on the same spot of graphene with increasing force setpoint. $V_b = 0.108V$. Top: Topography images. Bottom: Current images. The setpoint from left to right: $60nN, 70nN, 80nN, 90nN, 100nN$

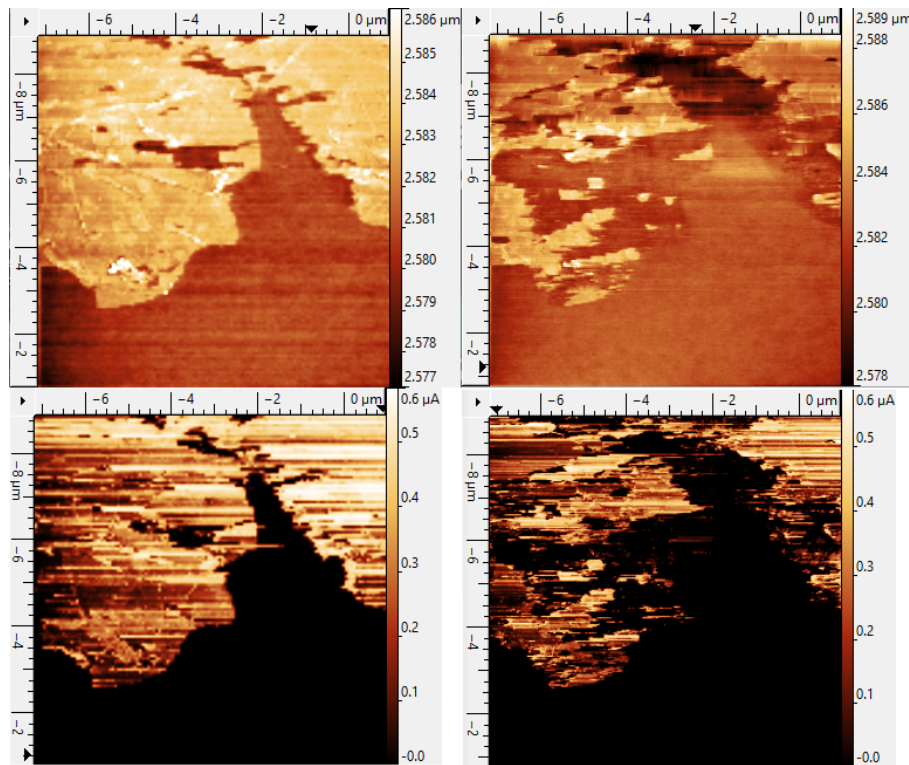


Figure 4.15: QI CAFM measurements on graphene taken right after each other. $V_b = 0.108V$, $sp = 92nN$ Left: Initial topography and current image, the graphene is clearly visible in both images. Right: Topography and current image taken right after the first one. Many graphene spots seemed to have disappeared, so graphene is being damaged.

sample and tip which were used. One should not use a setpoint too high though, because the high force can severely damage the tip. In the case of the RMN tips, a high setpoint can result the tip to bend. For tips made of metal coated Si, the metal can wear off. It was found that the optimal setpoint could be found by gradually increasing the load until a sufficient increase in current appeared all through the image. This is when the tip pushes through contamination layers. An example of this is shown in figure 4.14. In the first two images ($sp = 60nN, 70nN$, note that the forces are now given in Newton instead of Volt, due to a calibration for this specific tip) the tip does not push enough in order to even measure the graphene structure in the height image. A setpoint of $80nN$ apparently is enough for measuring the graphene structure in the height image, but the tip still did not push enough to make a clean contact with graphene in order to measure current. Current becomes visible around $90N$ and is fully visible on

the graphene at $100nN$. For this reason, setpoints used during this project for doing CAFM were mostly around the $90nN$ or $100nN$, which are quite high. Note that at around $100nN$ graphene starts to get damaged.

Though these tests make it seem that force setpoints with such high forces are optimal, many measurements would rise the suspicion that the force used was too high. Figure 4.15 shows two height and current images made just two minutes after each other with a force setpoint of $92nN$. Both in the height image and the current image it appears as if the graphene has changed significantly. This was more frequently observed in subsequent images while using these specific settings, regardless of which voltage. It could be caused by the tip pushing too heavily onto the graphene surface, changing its topography (damaging/cutting) while doing so. Especially since this occurred at the end of a graphene sheet, where graphene will have more defects[22] than in the middle of a sheet, which makes it weaker.

4.7 Conclusion

Knowing about this damaging effect, it would seem as if CAFM on graphene is really suboptimal, as it is possible to measure current on graphene and identify graphene, but only when such a high force is used so that the graphene itself changes, making measurements qualitatively a lot worse. The high force causes damage at the edges where it is more weak. This is a drawback, but it can be used to "cut" graphene by AFM nanolithography.

At the root of this problem lies a deeper issue. The reason that such a high force setpoint had to be used, was that the tip would have to push through contamination and adsorbate layers. Tip/sample contamination is a big drawback, as measurements would more often than not show no current in current images/curves. This proved to become more of an issue when samples were stored for longer, increasing the period in which the sample was exposed to air, thus increasing contamination. Using high forces would to some extent solve the problems of contamination, but impose other problems as mentioned above. Using fresh/new samples and recently cleaned tips (tips could be cleaned by argon etching for example) could decrease the amount of contamination. Also, improvements could be made by measuring in a more controlled atmosphere and storing the samples in a better vacuum (samples during this project were stored in a 1 mbar vacuum).

No conclusion could be made on the optimal CAFM resolution, because there was no time to push the limits of CAFM resolution.

For further research on CAFM, one might want to try using Si or SiN tips coated with conducting (doped) diamond or metal carbides or Titanium.

Acknowledgements

Special thanks to Liuba Belyaeva (group of G. Schneider, LIC.) for making the graphene samples used in this project. Also, thanks to the FMD for helping with technical difficulties, and the members of the Van Ruitenbeek-group for offering support during this project.

Bibliography

- [1] *graphenea.com*.
- [2] K. S. Novoselov, A. K. Geim, S. V. Morozov, D. Jiang, Y. Zhang, S. V. Dubonos, I. V. Grigorieva, and A. A. Firsov, *Electric Field Effect in Atomically Thin Carbon Films*, *Science* **306**, 666 (2004).
- [3] <https://www.researchtrends.com/issue-38-september-2014/graphene-ten-years-of-the-gold-rush/>.
- [4] C. Lee, X. Wei, J. W. Kysar, and J. Hone, *Measurement of the Elastic Properties and Intrinsic Strength of Monolayer Graphene*, *Science* **321**, 385 (2008).
- [5] <http://www.physics.upenn.edu/kane/pedagogical/295lec3.pdf>.
- [6] J.-H. Chen, C. Jang, S. Xiao, M. Ishigami, and M. S. Fuhrer, *Intrinsic and extrinsic performance limits of graphene devices on SiO₂*, *Nature Nanotechnology* **3**, 206 (2008).
- [7] A. Bellunato, S. D. Vrbica, C. Sabater, E. W. de Vos, R. Fermin, K. N. Kanneworff, F. Galli, J. M. van Ruitenbeek, and G. F. Schneider, *Dynamic Tunneling Junctions at the Atomic Intersection of Two Twisted Graphene Edges*, *Nano Letters* **0**, null (0), PMID: 29513997.
- [8] P. E. West, *Introduction to atomic force microscopy theory, practice, applications*, (2007).
- [9] Fowles and Cassiday, *Analytical Mechanics, seventh edition*.
- [10] F. Galli, *Lecture-notes-atomic-force-microscopy-2017-Federica-Galli*.

-
- [11] T. Tiedje and A. Brown, *Performance limits for the scanning tunneling microscope*, **649** (1990).
- [12] C. J. Chen and W. F. Smith, *Introduction to scanning tunneling microscopy*, *American Journal of Physics* **62**, 573 (1994).
- [13] J. Instruments, *JPK Conductive AFM (CAFM) module for NanoWizard ® AFM*, page 1.
- [14] V. Shahin, W. Hafezi, H. Oberleithner, Y. Ludwig, B. Windoffer, H. Schillers, and J. E. KÄEhn, *The genome of HSV-1 translocates through the nuclear pore as a condensed rod-like structure*, **119**, 23 (2006).
- [15] J. Instruments, *Quantitative Imaging with the NanoWizard*, page 1.
- [16] C. Science and N. Sciences, *Atomic Force Microscopy - An advanced physics lab experiment*, (2014).
- [17] *Rocky Mountain Technology, LLC*. <http://rmnano.com/index.html>.
- [18] P. Blake, E. W. Hill, A. H. Castro Neto, K. S. Novoselov, D. Jiang, R. Yang, T. J. Booth, and A. K. Geim, *Making graphene visible*, *Applied Physics Letters* **91** (2007).
- [19] S.-a. Peng, Z. Jin, P. Ma, D.-y. Zhang, J.-y. Shi, J.-b. Niu, X.-y. Wang, S.-q. Wang, M. Li, X.-y. Liu, T.-c. Ye, Y.-h. Zhang, Z.-y. Chen, and G.-h. Yu, *The sheet resistance of graphene under contact and its effect on the derived specific contact resistivity*, **82**, 500 (2015).
- [20] C. J. Muller, J. M. van Ruitenbeek, and L. J. de Jongh, *Conductance and supercurrent discontinuities in atomic-scale metallic constrictions of variable width*, *Phys. Rev. Lett.* **69**, 140 (1992).
- [21] M. K. Bles, A. W. Barnard, P. A. Rose, S. P. Roberts, K. L. McGill, P. Y. Huang, A. R. Ruyack, J. W. Kevek, B. Kobrin, D. A. Muller, and P. L. McEuen, *Graphene kirigami*, *Nature* **524**, 204 (2015).
- [22] A. J. M. Giesbers, U. Zeitler, S. Neubeck, F. Freitag, K. S. Novoselov, and J. C. Maan, *Nanolithography and manipulation of graphene using an atomic force microscope*, *Solid State Communications* **147**, 366 (2008).